

CAAP Annual Report

Date of Report: *10/12/2023*

Prepared for: *U.S. DOT Pipeline and Hazardous Materials Safety Administration*

Annual Period: **From** *(September 27, 2022)* **to** *(September 26, 2023)*

Contract Number: *693JK32250011CAAP*

Project Title: *Determination of Potential Impact Radius for CO₂ Pipelines using Machine Learning Approach*

Prepared by: *Sam Wang*

Contact Info.: *979-845-9803 & qwang@tamu.edu*

Table of Contents

| | |
|--|----|
| Table of Contents | 2 |
| Section A: Business and Activities | 3 |
| (a) Contract Activities | 3 |
| (b) Financial Summary | 3 |
| (c) Project Schedule Update | 4 |
| (d) Status Update of the 4 th Quarter Technical Activities | 4 |
| Section B: Detailed Technical Results in the Report Period | 5 |
| 1. Background and Objectives in the 1 st Annual Report Period | 5 |
| 1.1. Background | 5 |
| 1.2. Objectives in the 1 st Annual Report Period | 8 |
| 2. Studies in the 1 st Annual Report Period | 8 |
| 2.1. Potential Impact Radius for CO ₂ | 8 |
| 2.2. CFD model study | 10 |
| 2.2.1. Near-field stage by CFD | 11 |
| 2.2.2. Near-field stage by calculation | 14 |
| 2.3. Far-field stage | 19 |
| 2.4. Conditions for CO ₂ pipelines | 21 |
| 2.4.1. Parameters for CO ₂ pipelines | 21 |
| 2.4.2. Terrain | 21 |
| 2.5. Case Studies | 23 |
| 3. Future work | 26 |
| References | 27 |

Section A: Business and Activities

(a) Contract Activities

- Contract Modifications:

Contract was officially signed between PHMSA and Texas A&M University (then internally with Texas A&M Engineering Experiment Station)

- Educational Activities:

- Student mentoring: Pingfan Hu, Chi-Yang Li, Jazmine Aiya D. Marquez
- Student internship: None
- Career employed: Pingfan Hu received his PhD degree in May 2023 and now employed by Atlas Copco Power Technique North America

- Others:

- Dissemination of Project Outcomes: One peer-reviewed journal paper; Two public invited presentations: PRCI CO₂ Workshop in Orlando and ADMLC webinar hosted by Simon Gant at UK HSE.
- Citations of the Publications: C.-Y. Li, J.A.D. Marquez, P. Hu, Q. Wang, CO₂ pipelines release and dispersion: A review. *Journal of Loss Prevention in the Process Industries* **2023**, 85, 105177.

(b) Financial Summary

- Federal Cost Activities:

- PI/Co-PIs/students involvement: PI involvement with 0.75 month of time and efforts; Students with 9 months of time and efforts in total
- Materials purchased/travel/contractual (consultants/subcontractors): Subcontractor NFPA cost ~\$200 for organizing TAP meeting and taking meeting minutes; no materials purchase and travel cost

- Cost Share Activities:

- Cost share contribution: 1.25 months of PI's time and efforts. He devoted his time to supervise the graduate students, organize TAP meetings/kickoff meeting, work with NFPA and other TAP members, review all work, technical trouble shooting for CFD, and prepare the progress/annual reports.

(c) Project Schedule Update

- Project Schedule:

| Task | Year 1 | | | | Year 2 | | | |
|--|--------|----|----|----|--------|----|----|----|
| | Q1 | Q2 | Q3 | Q4 | Q1 | Q2 | Q3 | Q4 |
| Establish the CFD models of CO ₂ release and dispersion from a high-pressure pipeline | █ | █ | | | | | | |
| Construct the database of CO ₂ dispersion | | █ | █ | █ | █ | | | |
| Perform QPCR analysis and identify the PIR for CO ₂ pipelines | | | | | █ | █ | | |
| Develop a web-based tool to determine the PIR for CO ₂ pipelines and evacuation time for surrounding public | | | | | | | █ | █ |

- Corrective Actions: Task 1 took about 3 quarters and now we are constructing the database of CO₂ dispersion, which may take two more quarters to finish.

(d) Status Update of the 4th Quarter Technical Activities

- **Task 1:** Establish the CFD models of CO₂ release and dispersion from a high-pressure pipeline
 - 1.1: Summarize the physical models for CO₂ dispersion and the availability of CFD software that is applicable for CO₂ dispersion
 - 1.2: Summarize the CFD simulation results and the comparison of their computing efficiency, as well as the existing literature about how PIR was addressed
- **Task 2:** Construct the database of CO₂ dispersion under different scenarios
 - 2.1: Summarize the common CO₂ pipeline operating conditions and the dispersion parameters determined for CFD simulations
 - 2.2: Summarize the database for the PIR for CO₂ pipelines with different health consequences (*ongoing*)

Section B: Detailed Technical Results in the Report Period

1. Background and Objectives in the 1st Annual Report Period

1.1. Background

As global concern about climate change continues to grow, Carbon Capture, Utilization, and Storage (CCUS) applications are increasingly taking center stage in ongoing global discussions. Onyebuchi et al. (2018) claimed that pipelines are essential for conveying CO₂ to an appropriate sequestration site, especially when a consistent flow from the CO₂ capture facility is required. Furthermore, pipelines facilitate the economical and efficient conveyance of substantial volumes of CO₂ across extensive distances.

Nevertheless, comprehending the potential risks linked to CO₂ pipeline failures is vital for ensuring the feasibility and efficacy of CCUS as a solution to counteract the effects of global warming (Woolley et al., 2014). Although CO₂ is neither toxic nor flammable, its asphyxiant nature coupled with the catastrophic release from a pipeline rupture could still pose a significant threat. Witkowski et al. (2013) claimed that higher concentrations of carbon dioxide could negatively affect human behavior and health (Figure 1). A CO₂ concentration of 1% induces drowsiness and exceeding 2% can result in a mild narcotic effect. Concentrations between 3% and 5% hinder breathing, leading to dizziness and headaches. Exposure to levels above 10% may lead to loss of consciousness, with prolonged exposure potentially resulting in suffocation. CO₂ concentrations surpassing 20% can lead to immediate fatality. In 2020, a CO₂ pipeline accident occurred in Satartia, Mississippi, resulting in over 40 people requiring hospital treatments. Therefore, gaining insight into the consequences of CO₂ pipeline failures is vital for making CCUS a practical and effective solution for addressing global warming.

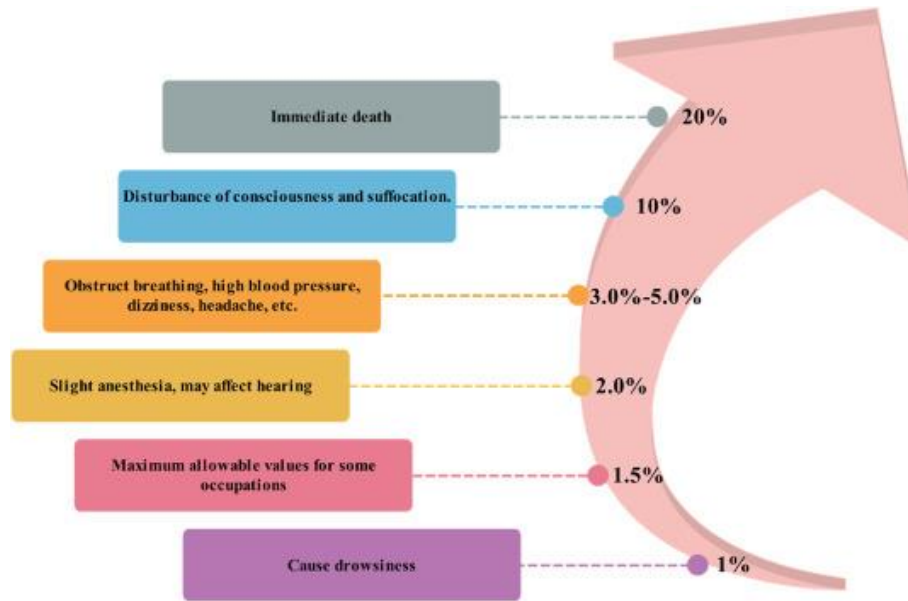


Figure 1. The negative impact of different CO₂ concentrations on human health (adopted from Lu et al. (2020)).

Assessing the potential impact radius of incidents involving the release of CO₂ from pipelines is a crucial step, achieved using reliable dispersion models. This assessment provides valuable insights into possible scenarios. By identifying and analyzing these scenarios, we can implement the requisite safety measures and develop an effective emergency response plan, ensuring the secure and responsible deployment of CCUS technology. However, the development of an accurate dispersion model hinges on data derived from CO₂ pipeline release experiments. Fortunately, numerous government agencies and joint industry projects have undertaken extensive large-scale CO₂ dispersion experiments. Their efforts lead to comprehensive investigations into the dispersion behavior of CO₂ resulting from pipeline ruptures and the acquisition of valuable experimental data for the development and validation of CO₂ dispersion models. Furthermore, the computational methods could update accordingly.

Computational Fluid Dynamics (CFD) is an advanced numerical simulation technique used to study the behavior of fluids as they interact with solids or other fluids. Consequently, intricate flow patterns and heat transfer can be replicated within virtual environments (Jiao et al., 2019; Z. Wang et al., 2016; Yi et al., 2019, 2020). Recently, there have been many applications on simulating CO₂ dispersion through CFD with reasonably good results (Godbole et al., 2018; Rian et al., 2014; Shen et al., 2020). For an accurate simulation of a scenario, it is essential to define appropriate geometry and set specific boundary conditions for CO₂ dispersion. To emulate turbulence effects and CO₂ behavior accurately, transport and thermodynamic models are selected. Since these models are constrained by the mathematical terms used to represent specific properties or behaviors, a comprehensive understanding of both experimental results and the system itself is necessary to choose the most suitable model. Depending on the scenario, additional factors such as weather conditions, phase change models, and particle dispersion models may be incorporated to enhance accuracy. Hence, CFD has the potential to offer precise predictions for CO₂ pipeline release dispersion, and corresponding potential impact radius (PIR).

While CFD can provide reasonably accurate predictions, it is important to acknowledge that the setup and execution of CFD simulations can be complex and time-consuming. As we strive for more efficient and quicker methods of prediction, the integration of machine learning models emerges as a promising solution. Machine learning can harness large datasets and learn from them to make predictions with speed and efficiency (Jiao et al., 2020). By feeding the model with the right set of parameters, we can achieve accurate and rapid predictions, making it a valuable complement to traditional CFD simulations. The synergy between CFD and machine learning holds the potential to significantly enhance our ability to assess and address various scenarios, including CO₂ dispersion, in a more efficient and effective manner.

1.2. Objectives in the 1st Annual Report Period

The primary objective of this project is to create a fast and widely applicable machine-learning based tool, based on simulations from CFD, for evaluating the outcomes of accidental CO₂ dispersion and establishing the PIR for CO₂ pipelines. Therefore, the proposed project will consist of four stages: (1) Establish the CFD models of CO₂ release and dispersion from a high-pressure pipeline; (2) Construct the database of CO₂ dispersion under different scenarios; (3) Perform QPCR analysis and identify the PIR for CO₂ pipelines; and (4) Develop a web-based tool to determine the PIR for CO₂ pipelines and evacuation time for the surrounding public. In this annual report, we mainly focus on Stage 1 and part of Stage 2.

2. Studies in the 1st Annual Report Period

2.1. Potential Impact Radius for CO₂

The calculation of the potential impact radius of the potential impact circle within which the potential failure of a pipeline could have a significant impact on people or property is the key step of the 49 CFR 192 Subpart O - Gas Transmission Pipeline Integrity Management. The specific formula for the PIR of natural gas is provided as:

$$r = 0.69\sqrt{p \cdot d^2}$$

Where, r is the PIR in feet, p is the maximum allowable operating pressure (MAOP) in the pipeline segment in pounds per square inch, and d is the nominal diameter of the pipeline in inches.

For the transporting gases other than natural gas, the operator should apply the different factors to calculate the corresponding PIR (Baker Jr, 2005).

$$r = \sqrt{\frac{14490 \cdot \mu \cdot \chi_g \cdot \lambda \cdot C_d \cdot H_C \cdot Q \cdot p \cdot d^2}{a_0 \cdot I_{th}}}$$

Where, r is the PIR in feet, μ is combustion efficiency factor, χ_g is emissivity factor, λ is release rate decay factor, C_d is discharge coefficient, H_C is heat of combustion in BTU per pound, Q is flow factor, p is the maximum allowable operating pressure (MAOP) in the pipeline segment in pounds per square inch, d is the nominal diameter of the pipeline in inches, a_0 is sonic velocity of gas in feet per second, and I_{th} is threshold heat flux in BTU per hour square feet.

However, the premise to apply these formulas is that thermal radiation from a sustained jet or trench fire is the dominant hazard for the pipe rupture because these formulas are derived from the fire model with the consideration of the threat to human life from the thermal radiation (Baker Jr, 2005; Stephens et al., 2002). To natural gas or other flammable gases whose specific gravity are significantly lower than air, gases could barely accumulate around the ground to form the vapor cloud, which could turn into vapor cloud explosion with the ignition source, so the application of these equations are valid. However, to the gases possessing hazardous characteristics with specific gravity around or higher than 1, the dispersion around the ground and concentration of the gases is the dominant hazard to the people and property, thus these equations could not be applied to calculate the PIR.

The hazardous characteristic for CO₂ is asphyxia and the specific gravity of CO₂ is higher than one, so we could not apply the above formula to determine the PIR for CO₂ pipelines. Therefore, we plan to combine computational fluid dynamics models and machine learning technique to develop a tool to determine the PIR for CO₂ pipelines.

2.2. CFD model study

Before starting on the establishment of the simulation model for CFD on the release from CO₂ pipelines, we conducted a literature review to identify the appropriate physical models and numerical methods to describe the release of high-pressure CO₂ (Li et al., 2023). Additionally, because there are many details for conducting simulation on Ansys Fluent, we went through many materials on Ansys Fluent training.

According to the work on the preparedness, the accurate prediction for CO₂ dispersion with SST $k-\omega$ turbulence model, Peng-Robinson equation of state and power law on wind velocity profile. Furthermore, separating the simulation scope to near-field stage and far-field stage is the widely used method on simulating the dispersion behavior from high-pressure CO₂ pipelines (Figure 2). In near-field stage, we analyze CO₂ depressurization behavior from the tanks or pipelines, while in far-field, we obtain the CO₂ dispersion results and CO₂ concentration profile afterwards.

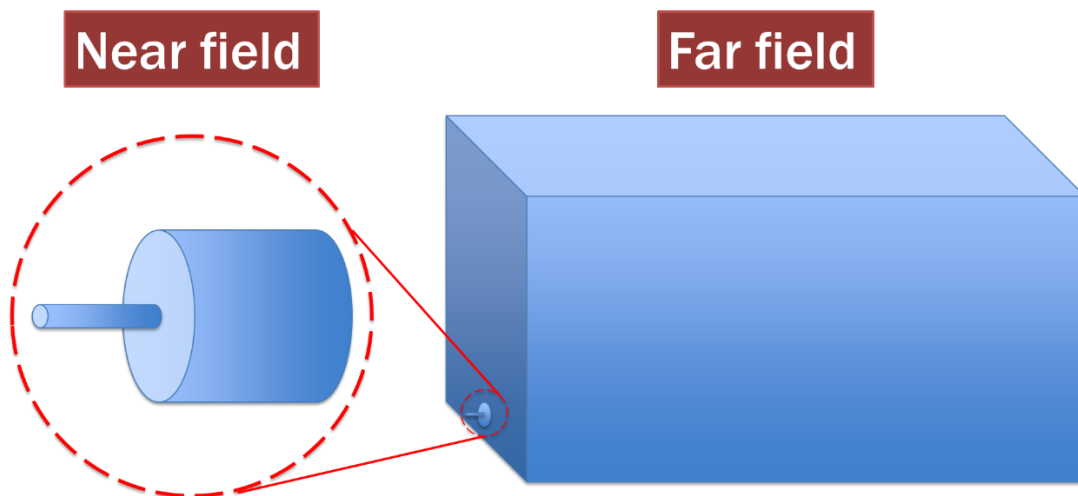


Figure 2. Near-field stage and far-field stage.

2.2.1. Near-field stage by CFD

In the near-field stage, the pressure drops rapidly, while temperature reduces accordingly, and velocity increases promptly. Thus, the behavior in the near-field stage is complicated. In Ansys Fluent, as the Mach number exceed 0.3, the density-based solver (rather than widely used pressure-based solver in most cases) is recommended to use. Therefore, we used the density-based solver for near-field stage and pressure-based solver for far-field stage.

Additionally, we need to obtain the length for near-field to set up the geometry for near-field stage and far-field stage. For the dispersion behavior from high pressure source, Mach disc (Figure 3) is a notable characteristic within specific shock wave occurrences, especially within the realm of swift supersonic or hypersonic flows. The distance of 10 times distance of Mach disc (x_m) is believed to be close to the ambient conditions and can be used for the simulation (Liu et al., 2014).

The equation of distance of Mach disc is as:

$$x_m = 0.6455 \times d_e \times \sqrt{\frac{P_0}{P_\infty}}$$

Where x_m is the distance of the Mach disc, d_e is the diameter of the nozzle exit, P_0 is the stagnation pressure, and P_∞ is the ambient pressure.

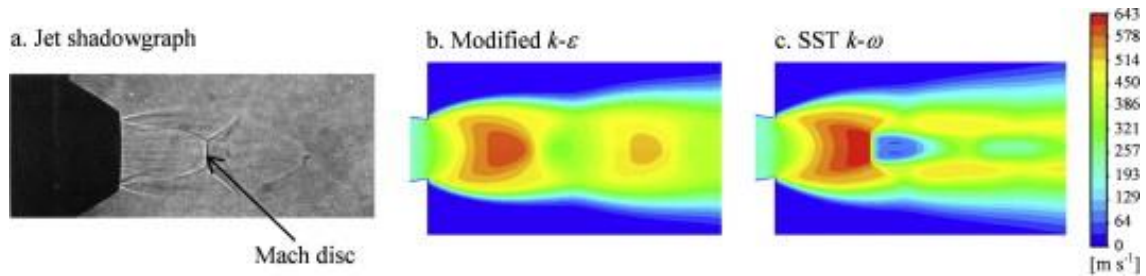


Figure 3. Mach disc (adopted from Liu et al., 2014).

Furthermore, because the complexity for the near-field stage, we applied very fine mesh to make sure the simulation could work without encountering errors. Meanwhile, we utilized 2-D axisymmetric model to simplify the computation process to reduce the time for simulation. Therefore, to study the model for the further utilization, we simulated the results of BP test 8 from CO2PIPETRANS JIP project; while the parameters used are as Table 1, the geometry and mesh is shown in Figure 4, and simulation results is shown in Figure 5.

Table 1. Parameters of BP test 8 near-field stage.

| Parameter | Value |
|----------------------------------|---|
| Orifice diameter (mm) | 11.94 |
| Pressure in the pipe (Pa) | 1.574×10^7 |
| Temperature in the pipe (K) | 420.3 |
| Ambient temperature (Pa) | 9.6×10^4 |
| Ambient pressure (K) | 281.0 |
| Wind velocity (m/s) | $5.51 \times \left(\frac{z}{8}\right)^{0.1168}$ |
| Distance of Mach disc, x_m (m) | 0.099 |

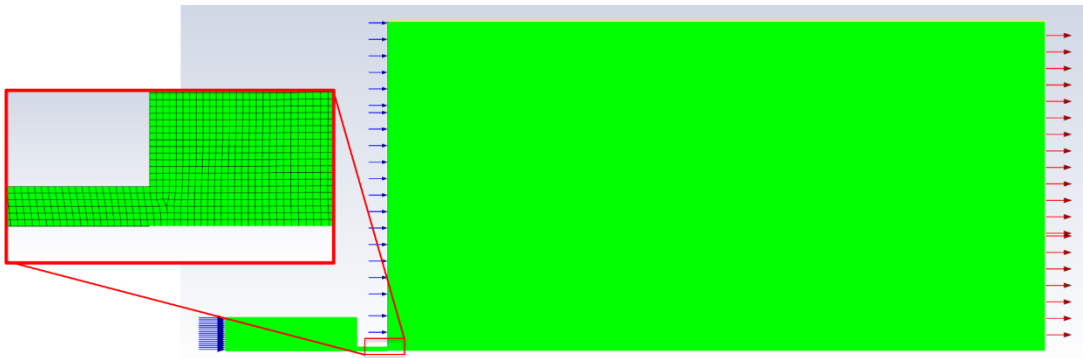


Figure 4. Geometry and mesh of BP test 8 near-field stage.

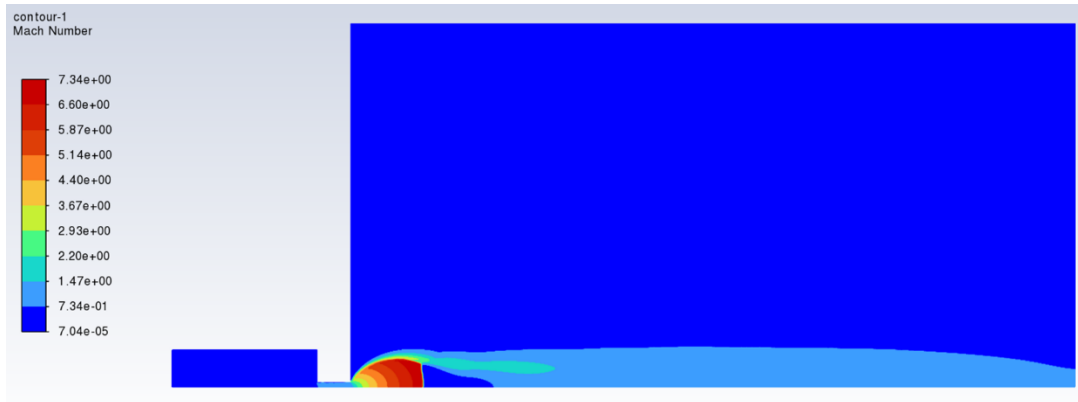


Figure 5. Simulation results of BP test 8 near-field stage.

From Figure 5, we could observe the Mach disc (Figure 3). Moreover, we also could get the accurate mass flow rate from this simulation (Figure 6), while the observed value was 4.07 kg/s (Witlox et al., 2014). Therefore, it could have very accurate prediction from CFD.

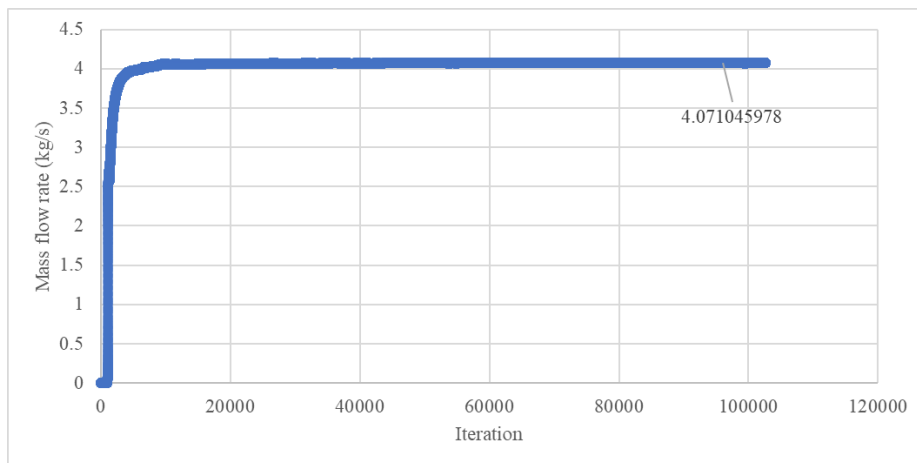


Figure 6. Mass flow rate from the near-field simulation.

However, the near-field stage for this relatively simple BP test 8 case took Texas A&M High Performance Research Computing (HPRC) a day to run the simulation, not to mention the CO₂ pipelines with higher pressure and temperature. Hence, it is expected to take significantly too much

time to create the database for our further machine learning step, so we need to adjust the procedure on predicting the near-field stage.

2.2.2. Near-field stage by calculation

Thus, we used the conservation equation of energy to do the calculation for near-field stage:

$$\Delta H + \Delta KE + \Delta PE = Q + W_s$$

Where, H is enthalpy, KE is kinetic energy, PE is potential energy, Q is heat, and W_s is shaft work.

$$\begin{aligned} & (m_a H_{a,i} + m_c H_{c,i} - m_a H_{a,f} - m_c H_{c,f}) + \left(\frac{1}{2} m_a v_{a,i}^2 + \frac{1}{2} m_c v_{c,i}^2 - \frac{1}{2} m_a v_f^2 - \frac{1}{2} m_c v_f^2 \right) + 0 \\ & = Q + W_s \end{aligned}$$

$$W_s = \Delta(P \times m_{c,e} \times V_m)$$

Where m_a is the mass flow of air, m_c is the mass flow of CO₂, $H_{a,i}$ is the enthalpy of air in initial state, $H_{c,i}$ is the enthalpy of CO₂ in initial state, $H_{a,f}$ is the enthalpy of air in final state, $H_{c,f}$ is the enthalpy of CO₂ in final state, $v_{a,i}$ is the velocity of air in initial state, $v_{c,i}$ is the velocity of CO₂ in initial state, v_f is the velocity of the mixture in final state, $m_{c,e}$ is the mass flow of escaped CO₂, and V_m is the specific volume of the CO₂.

For the W_s , Peng-Robinson equation of state and Joule-Thompson coefficient (μ_{JT}) applied to escaped CO₂ to calculate the shaft work on the surrounding based on isothermal expansion (Peng & Robinson, 1976; J. Wang et al., 2017).

$$P = \frac{RT}{V_m - b} - \frac{a\alpha}{V_m^2 + 2bV_m - b^2}$$

$$a = \frac{0.45724R^2T_c^2}{P_c}$$

$$b = \frac{0.07780RT_c}{P_c}$$

$$\alpha = \left(1 + (0.37464 + 1.54226\omega - 0.26992\omega^2)(1 - T_r^{0.5})\right)$$

$$T_r = \frac{T}{T_c}$$

Therefore, we could calculate the temperature and specific volume of CO₂ through the depressurization process. Consequently, we could calculate the shaft work per kilogram on surrounding by integrating the pressure difference from ambient pressure and specific volume, which is 248456.4 J/kg.

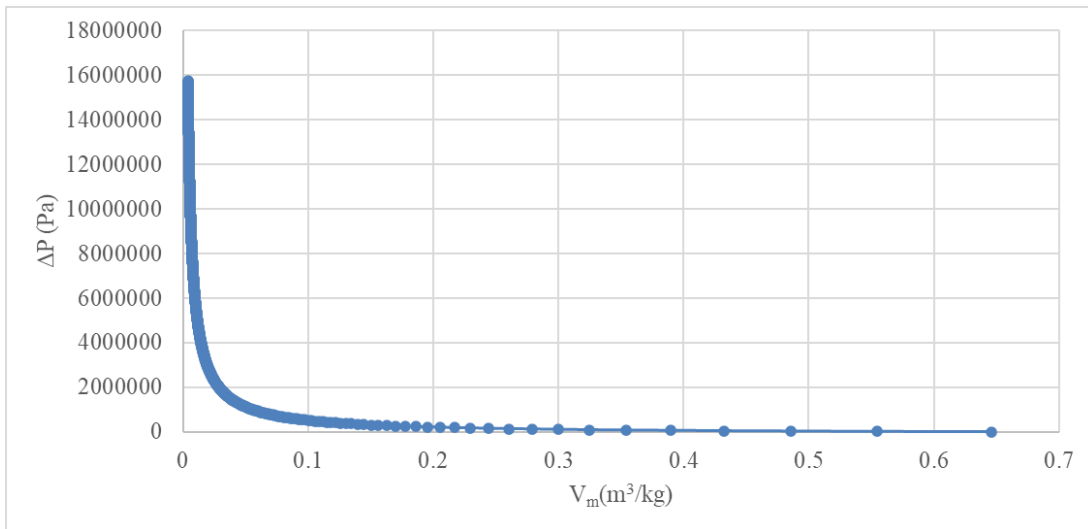


Figure 7. Shaft work of escaped CO₂.

Additionally, there is some heat loss from the dispersion. For this case, CO₂ will be passing through three sections before it is released into the atmosphere. From the storage tank, it will traverse a flexible hose, a metering spool, and an orifice plate (Table 2).

Table 2. The properties of the material.

| Transport path | Material | Length (m) | Inner radius (in) | Outer radius (in) | Thermal conductivity (W/m·K) |
|-----------------------|--|------------|-------------------|-------------------|------------------------------|
| Flexible hose | Hydrogenated Nitrile Butadiene Rubber (HNBR) | 3 | 2 | 1.25 | 0.23 |
| Metering spool (pipe) | Steel | 2 | 0.5 | 0.42 | 45 |
| Orifice plate | Stainless Steel | 0.5 | 0.5 | 2.2 | 15 |

These transport paths were based on common materials used for CO₂ transportation. To account for the heat lost from transport between the storage tank and the orifice, the heat generated by the fluid through each of the materials was calculated using the following equation:

$$Q = \frac{2\pi kL(T_i - T_o)}{\ln\left(\frac{r_o}{r_i}\right)}$$

Where, k is the thermal conductivity; L is the length of the pipe; T_i is the temperature inside the pipe; T_o is the temperature outside the pipe; r_o is the outer radius of the pipe; and r_i is the inner radius of the pipe. Hence, the heat loss from CO₂ transport can be summed as:

$$Q = Q_{FlexibleHose} + Q_{MeteringSpool} + Q_{OrificePlate}$$

Table 3 summarizes the heat loss from CO₂ transport.

Table 3. Heat loss from CO₂ transport in BP test 8.

| Material | Heat Loss (W) |
|----------------|---------------|
| Flexible Hose | 4,550.8 |
| Metering Spool | 144,688.8 |
| Orifice Plate | 2,706.4 |
| Total | 151,946 |

In the near-field stage, there is some fraction of CO₂ would disperse to surrounding, while some air entrains and mixes with CO₂. According to the near-field stage simulation from Ansys Fluent, 3.8 kg/s (out of total 4.07 kg/s CO₂ from the pipe) CO₂ blended with air and accounted for around 28.22 wt%. Therefore, m_c is 0.27 kg/s, which would conduct shaft work on surrounding. Additionally, there is also the heat loss from CO₂ transport. On the other hand, the initial state (420.3 K and 15.74 MPa) is the CO₂ in the pipe and some air in the ambient temperature with wind speed; the final state (281 K and 96000 Pa) is the mixture of CO₂ and air at the 10 times of the distance of Mach disc (x_m) from the pipe. Because shaft work and heat loss from pipe calculations are based on ideal conditions, we introduce 10 % more of them to do further calculations. With the equations below, we could calculate the required parameter used for the far-field.

$$\rho_{mix} = \frac{PM_{mix}}{RT}$$

$$A_f = \frac{m_a + m_c}{\rho_{mix}v_f}$$

Where ρ_{mix} is the density of mixture, P is the pressure, M_{mix} is the molecular weight of mixture, R is the gas constant, T is the temperature, and A_f is the input area of far-field stage.

With the equations mentioned above, we could get the velocity, composition of CO₂, and area from the near-field stage (Table 4). Thus, we could use them in the far field to simulate the dispersion behavior.

Table 4. Parameters obtained from near-field stage.

| Parameter | Value |
|------------------------|-------|
| Mass fraction (%) | 28.22 |
| Velocity (m/s) | 21.33 |
| Area (m ²) | 0.46 |

2.3. Far-field stage

With the parameters from Table 4, we could conduct the simulation for far-field stage to investigate CO₂ concentration versus the distance. For the far-field stage, the geometry and mesh for the scope is as Figure 8. The CO₂ concentration contours is shown in Figure 9. The CO₂ concentration along the downstream is as Figure 10. The comparison of experimental results and current simulation results is shown in Table 5.

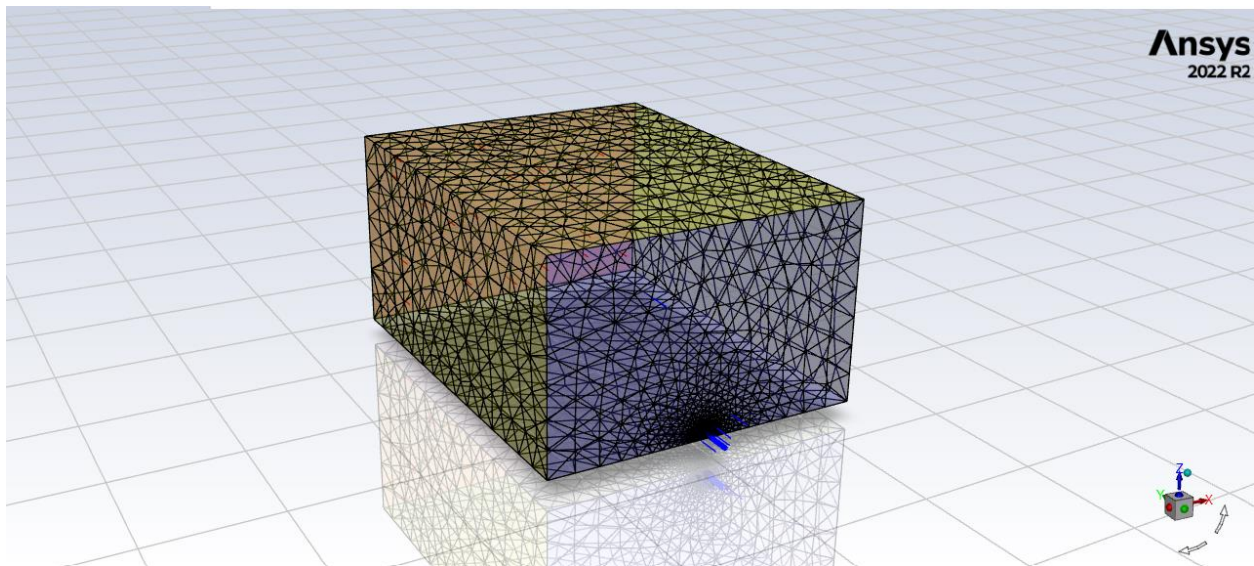


Figure 8. Geometry and mesh for the scope of simulation.



Figure 9. CO₂ concentration contours.

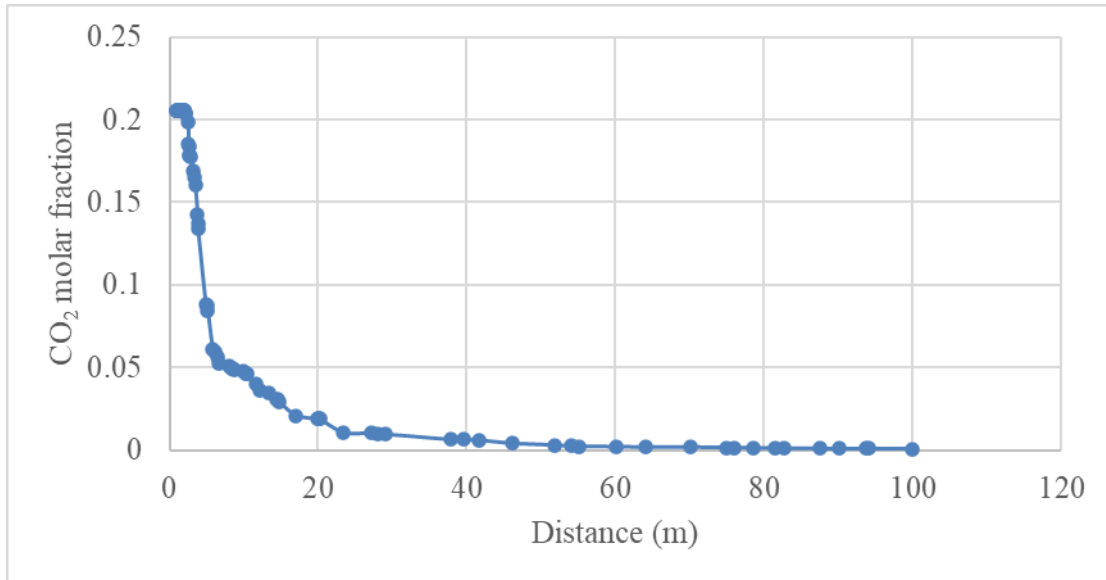


Figure 10. The CO₂ molar fraction along the downstream for BP test 8.

Table 5. The comparison of CO₂ concentrations between experiments and simulations.

| Downstream distance from source (m) | Highest molar fraction (%) | |
|--|----------------------------|------------|
| | Experiment | Simulation |
| 5 | 8.22% | 8.69% |
| 10 | 3.36% | 3.52% |
| 20 | 1.85% | 1.61% |
| 40 | 1.49% | 0.70% |

The sensors for 5, 10, and 20 meters are located 1 meter above the ground, while the sensor for 40 meters is located 0.3 meter above the ground. From Table 5, we can find CO₂ concentrations are accurate at 5, 10, and 20 meters, but not at 40 meters. Because the 40 meters one is further and lower than others are, the influence of the terrain would be higher than others. In the simulation, we could not access the terrain information, so we just used the flat surface. Perhaps, this is some terrain could accumulate CO₂ around ground, which led the higher concentration. This is a potential reason for the error.

2.4. Conditions for CO₂ pipelines

2.4.1. Parameters for CO₂ pipelines

To create the database for the machine-learning model, we are going to conduct CFD simulations base on the practices of CO₂ pipelines. The parameters are as (Knoope et al., 2013; National Energy Technology Institute, 2015).

Table 6. The variables for pipeline characteristics and weather conditions

| | Variable | High | Medium | Low |
|--------------------------|-------------------|------|--------|-----|
| Pipeline characteristics | pressure (MPa) | 20 | 10 | 1 |
| | diameter (inch) | 30 | 16 | 4 |
| | flow rate (MMcfd) | 1300 | 590 | 30 |
| Weather conditions | wind speed (mph) | 25 | 12 | 1 |
| | temperature (°F) | 100 | 60 | 0 |

2.4.2. Terrain

The terrains where CO₂ pipelines might locate could be roughly classified into 5 categories, including plain, moderate slope, steep slope, valley with moderate slope, and valley with steep slope. To simulate the CO₂ dispersion with real terrains, the geometries in Monticello Mississippi (Figure 11), Raton New Mexico (Figure 12), Walsenburg Colorado (Figure 13), Vernal Utah (Figure 14), and Calistoga California (Figure 15) were chosen to represent these 5 categories (National Energy Technology Institute, 2015).

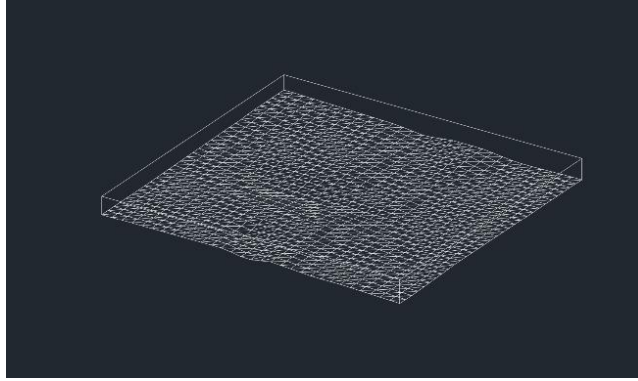


Figure 11. Monticello Mississippi

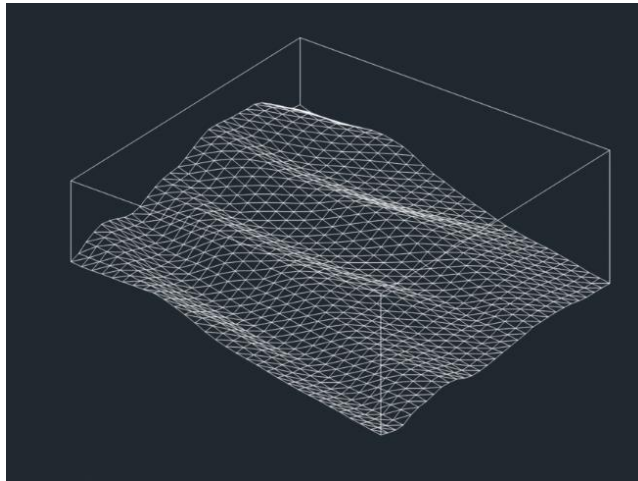


Figure 12. Raton New Mexico

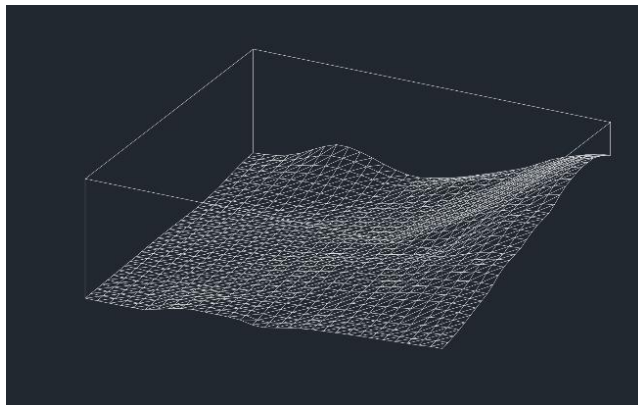


Figure 13. Walsenburg Colorado

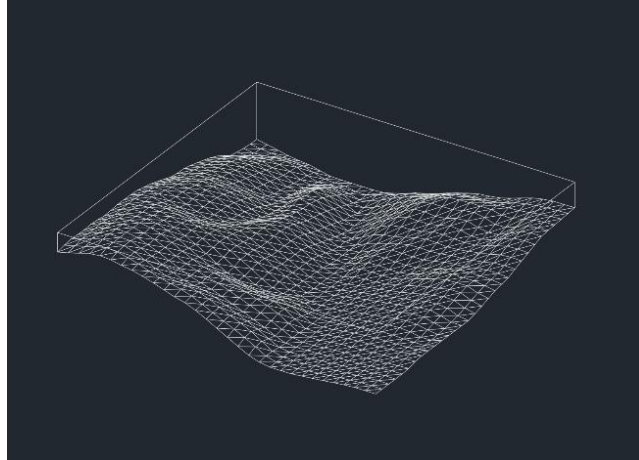


Figure 14. Vernal Utah

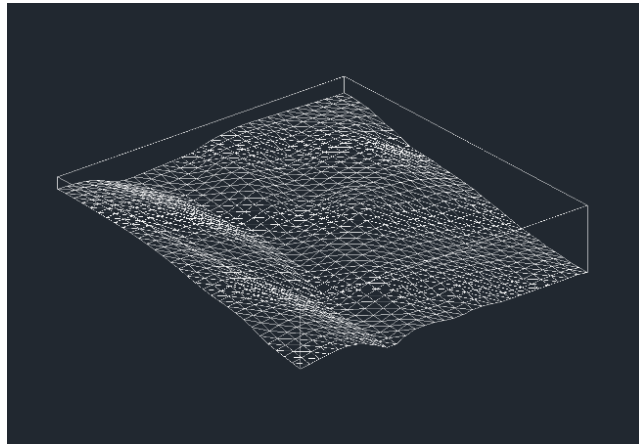


Figure 15. Calistoga California

2.5. Case Studies

Two case studies (Table 7) have been conducted based on the above-mentioned method, which is the combination of calculation on near-field and CFD simulation on far-field.

Table 7. Parameters for two case studies.

| | Variable | Case 1 | Case 2 |
|--------------------------|-------------------|--------|--------|
| Pipeline characteristics | pressure (MPa) | 20 | 20 |
| | diameter (inch) | 4 | 30 |
| | flow rate (MMcfd) | 30 | 1300 |
| Weather conditions | wind speed (mph) | 1 | 1 |
| | temperature (°F) | 60 | 60 |

The CO₂ concentration along the downstream and the distance for CO₂ concentration at 1%, 4%, and 9% are shown in Figures 16 and 17, and **Error! Reference source not found..**

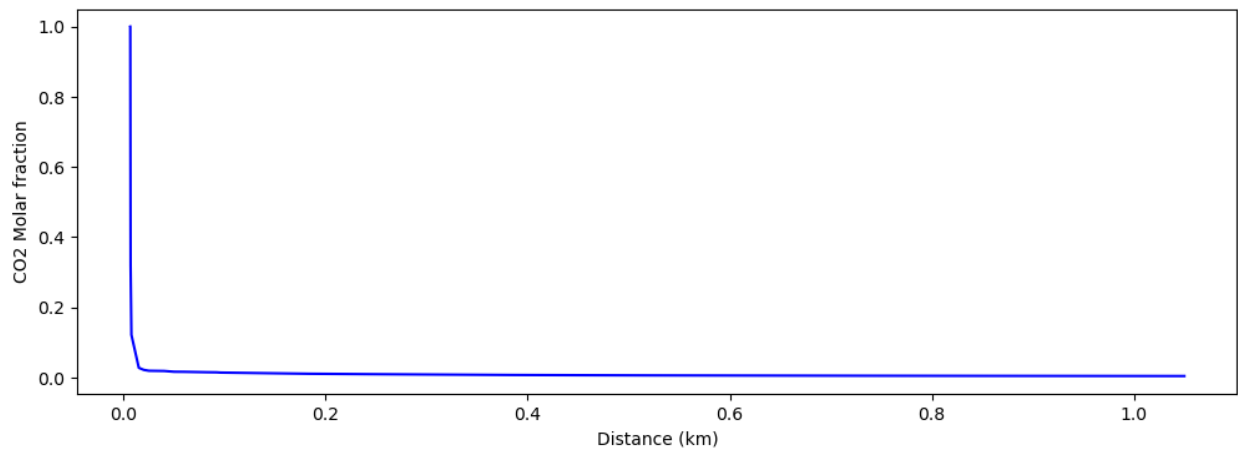


Figure 16. The CO₂ concentration along the downstream for Case 1.

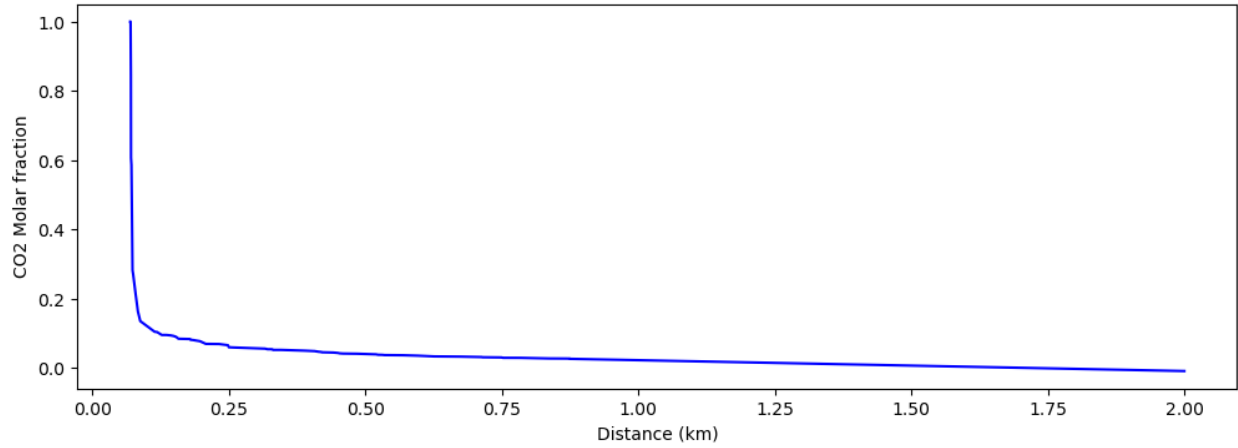


Figure 17. The CO₂ concentration along the downstream for Case 2.

Table 8. The distance for CO₂ concentration at 1%, 4%, and 9%.

| Concentration | 1% | 4% | 9% |
|---------------|------|-----|-----|
| Case 1 | 210 | 10 | 6 |
| Case 2 | 1810 | 450 | 155 |

Subsequently, we could create the database for machine learning based on this method.

3. Future work

- Perform parametric studies using Texas A&M HPRC for all dispersion scenarios by using Ansys Fluent with the numeric simulation setup mentioned above. For other parameters of concern, besides the 5 categories of terrains, the variables for pipeline characteristics and weather conditions are summarized in Table 6 (updated after recommendations from technical advisory panel).
- Create the database for the PIR for CO₂ pipelines dispersion based on the simulation results with the setup above.
- Perform parametric studies to search for the suitable machine learning techniques and corresponding hyperparameters for the machine-learning model.

References

- Baker Jr, M. (2005). *TTO Number 13 Integrity Management Program Delivery Order DTRS56-02-D-70036 Potential Impact Radius Formulae for Flammable Gases Other Than Natural Gas Subject to 49 CFR 192 FINAL REPORT TTO Number 13 Potential Impact Radius Formulae for Flammable Gases Other Than Natural Gas*.
<https://rosap.ntl.bts.gov/view/dot/16991>
- Godbole, A., Liu, X., Michal, G., Lu, C., & Medina, C. H. (2018). *CO2SAFE-ARREST: A Full-Scale Burst Test Research Program for Carbon Dioxide Pipelines -- Part 3: Dispersion Modelling*. <http://asmedigitalcollection.asme.org/IPC/proceedings-pdf/IPC2018/51876/V002T07A020/2511356/v002t07a020-ipc2018-78530.pdf>
- Jiao, Z., Hu, P., Xu, H., & Wang, Q. (2020). Machine learning and deep learning in chemical health and safety: A systematic review of techniques and applications. In *ACS Chemical Health and Safety* (Vol. 27, Issue 6, pp. 316–334). <https://doi.org/10.1021/acs.chas.0c00075>
- Jiao, Z., Yuan, S., Ji, C., Mannan, M. S., & Wang, Q. (2019). Optimization of dilution ventilation layout design in confined environments using Computational Fluid Dynamics (CFD). *Journal of Loss Prevention in the Process Industries*, 60, 195–202.
<https://doi.org/10.1016/j.jlp.2019.05.002>
- Knoope, M. M. J., Ramírez, A., & Faaij, A. P. C. (2013). A state-of-the-art review of techno-economic models predicting the costs of CO₂ pipeline transport. *International Journal of Greenhouse Gas Control*, 16, 241–270. <https://doi.org/10.1016/j.ijggc.2013.01.005>
- Li, C. Y., Marquez, J. A. D., Hu, P., & Wang, Q. (2023). CO₂ pipelines release and dispersion: A review. *Journal of Loss Prevention in the Process Industries*, 85.
<https://doi.org/10.1016/j.jlp.2023.105177>
- Liu, X., Godbole, A., Lu, C., Michal, G., & Venton, P. (2014). Source strength and dispersion of CO₂ releases from high-pressure pipelines: CFD model using real gas equation of state. *Applied Energy*, 126, 56–68. <https://doi.org/10.1016/j.apenergy.2014.03.073>
- Lu, H., Ma, X., Huang, K., Fu, L., & Azimi, M. (2020). Carbon dioxide transport via pipelines: A systematic review. In *Journal of Cleaner Production* (Vol. 266). Elsevier Ltd.
<https://doi.org/10.1016/j.jclepro.2020.121994>
- National Energy Technology Institute. (2015). *A Review of the CO₂ Pipeline Infrastructure in the*
- Onyebuchi, V. E., Kolios, A., Hanak, D. P., Biliyok, C., & Manovic, V. (2018). A systematic review of key challenges of CO₂ transport via pipelines. In *Renewable and Sustainable Energy Reviews* (Vol. 81, pp. 2563–2583). Elsevier Ltd.
<https://doi.org/10.1016/j.rser.2017.06.064>
- Peng, D.-Y., & Robinson, D. B. (1976). A New Two-Constant Equation of State. *Industrial &*

- Engineering Chemistry Fundamentals*, 15(1), 59–64. <https://doi.org/10.1021/i160057a011>
- Rian, K. E., Grimsmo, B., Lakså, B., Vembe, B. E., Lilleheie, N. I., Brox, E., & Evanger, T. (2014). Advanced CO₂ dispersion simulation technology for improved CCS safety. *Energy Procedia*, 63, 2596–2609. <https://doi.org/10.1016/j.egypro.2014.11.282>
- Shen, R., Jiao, Z., Parker, T., Sun, Y., & Wang, Q. (2020). Recent application of Computational Fluid Dynamics (CFD) in process safety and loss prevention: A review. In *Journal of Loss Prevention in the Process Industries* (Vol. 67). Elsevier Ltd. <https://doi.org/10.1016/j.jlp.2020.104252>
- Stephens, M. J., Leewis, K., & Moore, D. K. (2002). *A Model for Sizing High Consequence Areas Associate with Natural Gas Pipelines*. http://asmedigitalcollection.asme.org/IPC/proceedings-pdf/IPC2002/36207/759/4549948/759_1.pdf
- Wang, J., Wang, Z., & Sun, B. (2017). Improved equation of CO₂ Joule-Thomson coefficient. *Journal of CO₂ Utilization*, 19, 296–307. <https://doi.org/10.1016/j.jcou.2017.04.007>
- Wang, Z., Wang, W., & Wang, Q. (2016). Optimization of water mist droplet size by using CFD modeling for fire suppressions. *Journal of Loss Prevention in the Process Industries*, 44, 626–632. <https://doi.org/10.1016/j.jlp.2016.04.010>
- Witkowski, A., Rusin, A., Majkut, M., Rulik, S., & Stolecka, K. (2013). Comprehensive analysis of pipeline transportation systems for CO₂ sequestration. Thermodynamics and safety problems. *Energy Conversion and Management*, 76, 665–673. <https://doi.org/10.1016/j.enconman.2013.07.087>
- Witlox, H. W. M., Harper, M., Oke, A., & Stene, J. (2014). Phast validation of discharge and atmospheric dispersion for pressurised carbon dioxide releases. *Journal of Loss Prevention in the Process Industries*, 30(1), 243–255. <https://doi.org/10.1016/j.jlp.2013.10.006>
- Woolley, R. M., Fairweather, M., Wareing, C. J., Falle, S. A. E. G., Mahgerefteh, H., Martynov, S., Brown, S., Narasimhamurthy, V. D., Storvik, I. E., Sælen, L., Skjold, T., Economou, I. G., Tsangaris, D. M., Boulougouris, G. C., Diamantonis, N., Cusco, L., Wardman, M., Gant, S. E., Wilday, J., ... Jamois, D. (2014). CO₂PipeHaz: Quantitative hazard assessment for next generation CO₂ pipelines. *Energy Procedia*, 63, 2510–2529. <https://doi.org/10.1016/j.egypro.2014.11.274>
- Yi, H., Feng, Y., Park, H., & Wang, Q. (2020). Configuration predictions of large liquefied petroleum gas (LPG) pool fires using CFD method. *Journal of Loss Prevention in the Process Industries*, 65. <https://doi.org/10.1016/j.jlp.2020.104099>
- Yi, H., Feng, Y., & Wang, Q. (2019). Computational fluid dynamics (CFD) study of heat radiation from large liquefied petroleum gas (LPG) pool fires. *Journal of Loss Prevention in the Process Industries*, 61, 262–274. <https://doi.org/10.1016/j.jlp.2019.06.015>